Calculation model for adhesive-bonded cross-laminated timber concrete composite elements
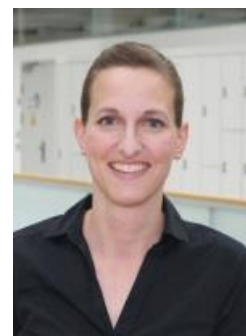
Georg Erlinger
FH Oberösterreich
Wels, Austria

Christoph Hackspiel
Camillo Sitte Bautechnikum Wien
Wien, Austria

FH-Prof. DI Dr. Karin Nachbagauer
FH Oberösterreich
Wels, Austria

Calculation model for adhesive-bonded cross-laminated timber concrete com-posite elements

1.　Abstract

In a timber-concrete composite the concrete takes over the pressure and the timber the tensile forces. The connection between the two materials often done by means of screws or notches, transmits the shear forces. This paper presents two calculation models for **adhesive**-bonded cross-laminated timber concrete composite elements. The first model accounts for the calculation of the ultimate limit state and the second one for the service-ability limit state. The basis of these two models is the γ-method. Climatic changes in temperature and the relative humidity of the environment are considered in the analysis of the long-term-behaviour.

The material parameters for concrete were taken from ÖNORM EN 1992-1-1. For the adhesive, tests were carried out to determine the exact shear modulus. The time depended behaviour of timber is described using a rheological model. Since the material behaviour of timber is highly influenced by the moisture content, its accurate calculation is of great importance. Therefore, the moisture content was determined with the implicit difference method using Fick´s law.

To validate the ULS Model, composite elements were loaded until failure. The recalculation has shown, that although the load is overestimated, the system rigidity can be predicted relatively well.

For the validation of the SLS Model, three composite slabs were loaded over a period of one year. The comparison with the calculation model shows, that the deformation behaviour can be predicted as well.

2.　Introduction

The bonding technology have been used in many sections of our general life since many centuries. Therefore, in an economic and static view it makes sense to produce bonded timber concrete composite (TCC) elements. In this paper, two calculation models for those elements are presented. This is intended to contribute to the development of TCC systems.

3.　Calculation Approaches

In the following section the calculation approaches, material-models, and methods which are integrated in the calculation models are presented.

3.1.　Gamma-Method

This method is the basis for both models and was developed by Möhler [1] for the calcu-lation of timber beams made out of single cross-sections connected elastically. It can be used analogous for TCC elements. The requirements for the usage of the γ-method are as follows: [2]

− Simple supported beam
− Uniform cross section
− Smeared connection
− Sinusoidal load

The sinusoidal load is in total almost like a uniformly distributed load. Hence, the method can be used for uniformly distributed loads with a negligible error. The following equations are for the calculation of a TCC element consisting of five parts – two longitudinal-, one cross-slat, one adhesive layer and a concrete slab. To describe the resilient connection on the second layer, the γ-values are used. γ_1 is calculated with equation (1) and refers to the concrete section. The second layer is held mental, because of that the value of γ_2 is

one. A value of one means rigid connection, whereas a value of zero means no connection. As a result, both the resilience of the composite joint and the traverse position in the cross laminated timber can be represented. The value γ3 is calculated with equation (2):

$$\gamma_1 = \left(1 + \frac{\pi^2 E_1 A_1}{l_{ref}^2} \cdot \frac{d_{1,2}}{b \, G_{R,12}}\right)^{-1} \tag{1}$$

$$\gamma_3 = \left(1 + \frac{\pi^2 E_3 A_3}{l_{ref}^2} \cdot \frac{d_{2,3}}{b \, G_{R,23}}\right)^{-1} \tag{2}$$

In these equations E_1 denotes the modulus of elasticity of the concrete and A_1 the corresponding concrete cross-sectional area. The area is calculated by multiplying the height d_1 by the width of the composite cross-section b, which is identical for all the layers. E_3 and A_3 refer to the longitudinal slat 3 of the CLT cross-section. The reference length l_{ref} corresponds to the span of a simple supported beam. The adhesive layer thickness is denoted by $d_{1,2}$ and the associated shear modulus by $G_{R,12}$.

Figure 1 shows the definition of the distances on the composite element. The layer 2 is the first layer of the CLT plate and the layer 3 is the bottom layer. Layer 2,3 represents the shear-soft transverse layer of the CLT.
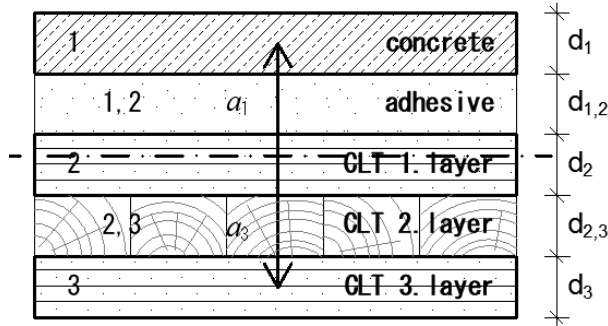

Figure 1: Assembly and definitions of a bonded timber-concrete element according to the Gamma-method.

The distances a_i are calculated with the equations (3), (4) and (5). [3]

$$a_2 = \frac{\gamma_1 \frac{E_1}{E_c} A_1 \left(\frac{d_1}{2} + d_{1,2} + \frac{d_2}{2}\right) - \gamma_3 \frac{E_3}{E_c} A_3 \left(\frac{d_2}{2} + d_{2,3} + \frac{d_3}{2}\right)}{\sum_{i=1}^{3} \gamma_i \frac{E_i}{E_c} A_i} \tag{3}$$

$$a_1 = \left(\frac{d_1}{2} + d_{1,2} + \frac{d_2}{2}\right) - a_2 \tag{4}$$

$$a_3 = \left(\frac{d_2}{2} + d_{2,3} + \frac{d_3}{2}\right) + a_2 \tag{5}$$

E_c denotes the reference module, which can be chosen arbitrarily. It makes sense to equate the reference module with the modulus of elasticity of the CLT since the factor E_i/E_c in the CLT thus becomes one. In principle, the moment of inertia is calculated as for a homogeneous cross section, but the layers are weighted with the stiffness ratios and the Steiner content is additionally reduced with the gamma factor.

$$J_{eff} = \sum_{i=1}^{3} \frac{E_i}{E_c} J_i + \sum_{i=1}^{3} \gamma_i \frac{E_i}{E_c} A_i a_i^2 \tag{6}$$

3.2. Moisture distribution in timber

To calculate the moisture u in the timber, Fick´s law was used for transient one-dimensional diffusion in the x-direction. [4]

$$\frac{\partial u}{\partial t} = D\, \frac{\partial^2 u}{\partial x^2} \tag{7}$$

The preceding equation (7) can be derived from the mass flow q from [4]:

$$q = -D \cdot \nabla c \tag{8}$$

Where c is the concentration of water that can be assumed to be proportional to the moisture content u, and D is the diffusion tensor. This tensor has only diagonal entries, namely the coefficients of diffusion between the individual layers. For the calculation of the coefficient of diffusion D(u) there are several approaches. The approach to Hanhijärvi [4] for spruce wood depends only on the moisture content of the wood u and is calculated as:

$$D(u) = 8{,}0 \cdot 10^{-11} \cdot e^{4{,}0\,u} \;\; [m^2/s] \tag{9}$$

Since the coefficient of diffusion D(u) is dependent on the wood moisture u, this has the effect that at a higher wood moisture leads to the increase in the diffusion of the wood. This causes a faster transport of moisture through the wood. Conversely, at a lower wood moisture the diffusion and the moisture transport speed are lower. The calculation of the moisture in the layers would be nonlinear, since the diffusion coefficient changes in each layer. However, the wood moisture changes only in small steps and D(u) is a very small number. Therefore, the coefficient of diffusion can be assumed to be constant with a negligible error.

Equation (7) can be solved for u = u (x, t) using the implicit difference method. In this case, the moisture u (x_i, t_m) in each wood layer x_i is determined at each time t_m. Equation (7) is approximated by means of difference quotients as follows:

$$
\begin{aligned}
\frac{u(x_i, t_{m+1}) - u(x_i, t_m)}{t_{m+1} - t_m} \\
= D\left(u\left(x_{i-1,i}, t_{m+1}\right)\right) \frac{u(x_{i-1}, t_{m+1}) - u(x_i, t_{m+1})}{(x_{i-1} - x_i)^2} \\
- D\left(u\left(x_{i,i+1}, t_{m+1}\right)\right) \frac{u(x_i, t_{m+1}) - u(x_{i+1}, t_{m+1})}{(x_i - x_{i+1})^2}
\end{aligned}
\tag{10}
$$

Whereby the coefficient of diffusion of layer x_i on layer x_{i+1} at time t_{m+1} is abbreviated to $D\left(u\left(x_{i,i+1}, t_{m+1}\right)\right) =: D_{i,m+1}$. For equidistant time and slice discretization, a simplified notation of $t_{m+1} - t_m = \Delta t$ and $x_i - x_{i+1} = \Delta x$ and $d_{i,m+1} = \frac{D_{i,m+1}\Delta t}{(\Delta x)^2}$ are used to represent equation (10) as:

$$u_{i,m+1} - u_{i,m} = d_{i-1,m+1}(u_{i-1,m+1} - u_{i,m+1}) - d_{i,m+1}(u_{i,m+1} - u_{i+1,m+1}) \tag{11}$$

If we rearrange equation (11) so that all quantities at time t_{m+1} are on the same side of the equation, the result is:

$$u_{i,m+1} - d_{i-1,m+1}u_{i-1,m+1} + d_{i-1,m+1}u_{i,m+1} + d_{i,m+1}u_{i,m+1} - d_{i,m+1}u_{i+1,m+1} = u_{i,m} \tag{12}$$

This equation must hold for each layer x_i for i = 1, 2, ... n-1 and thus results in a linear equation system with the unknowns $u_{i,m+1}$ for i = 1, 2, ... n-1 at the time t_{m+1}. For the efficient solution of the linear system of equations, care must be taken that the correct sorting of the layers produces a tridiagonal matrix and is sparse. In addition, the following conditions must be considered for the right-hand side of the linear system of equations:

The moisture of the layer n is equal to the moisture in the layer n-2 due to symmetry conditions. At the edge of the board, the moisture content of the wood is equal to the compensation humidity u_{RH}, which depends on the environment.

In Figure 2, the half of a board cross-section is shown for illustrative purposes. Details are described in the work of Fortuin [5] in chapter 4.1.
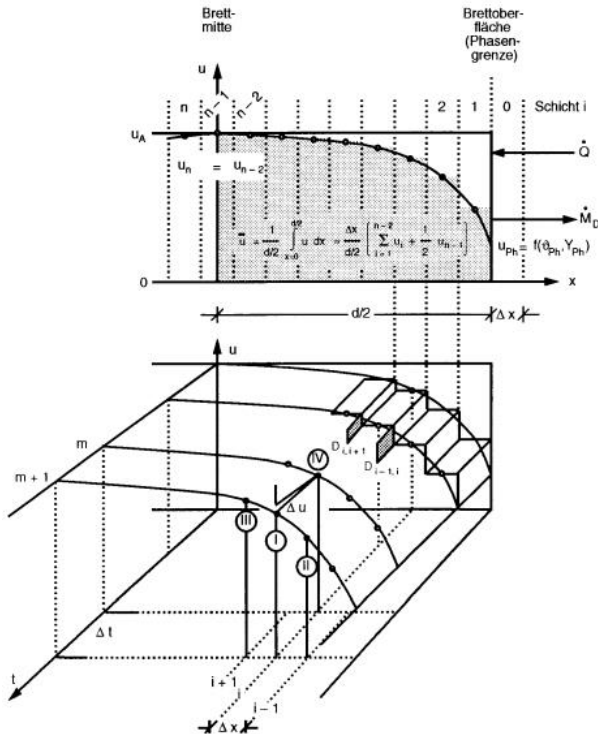

Figure 2: Moisture distribution in the wood cross-section with the implicit difference method [5]

3.3. Material-model for CLT

In this work the model of Eisenhut [6] was used for the modelling of the cross laminated timber. This corresponds to the material model according to Fortino [7] which was extended by the proportion of the thermal expansion α_T. Figure 3 shows the model.
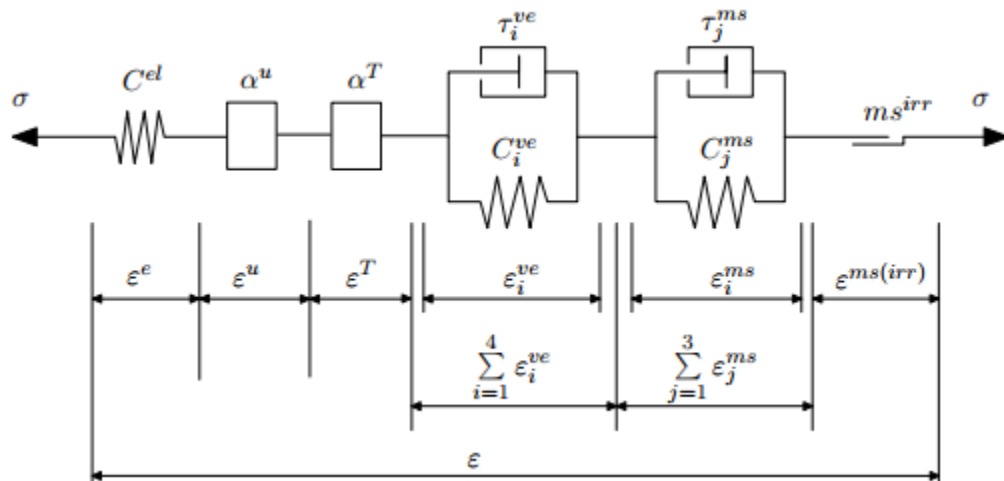

Figure 3: Material model by Fortino, extended by the temperature term α^T [6]

The total distortion is calculated using equation (13) and is dependent on the time t, the temperature T and the wood moisture u.

$$\varepsilon = \varepsilon^e + \varepsilon^u + \varepsilon^T + \sum_{i=1}^{4} \varepsilon_i^{ve} + \sum_{j=1}^{3} \varepsilon_j^{ms} + \varepsilon^{ms,irr} \tag{13}$$

with:

ε^e elastic strains

ε^u expansion due to moisture

ε^T expansion due to temperature

ε_i^{ve} viscoelastic strains

ε_j^{ms} mechano-sorptive strains

$\varepsilon^{ms,irr}$ irreversible mechano-sorptive strains

For the calculation of the individual terms refer to [6]. For the development of the long-term behaviour model, the viscoelastic and mechano-sorptive values of Fortino [7] and not of Eisenhut were used.

The creep number for the CLT is calculated to:

$$\varphi_{BSP,n-1} = \frac{\varepsilon(t)_{n-1}}{\varepsilon_0^e} - 1 \tag{14}$$

The elastic initial strain ε_0^e is calculated by dividing the stress by the modulus of elasticity at time t = 0. With an increase in load, the initial strain must be recalculated, as the stress also increases. The total strain is calculated using equation (13) and changes with time. Since the strains in the calculation model have some unrealistic outliers and these lead to rashes in the calculation, the creep was limited. The lower limit was set -0.1 and should allow the wood to increase the modulus of elasticity when, e.g., the ambient humidity decreases. At the top, the creep number was limited to 1.0 (see Wallner-Novak [3]).

4.   Development of the calculation models

Both calculation models for the adhesive composite of CLT and concrete are based on the γ-method. However, this was modified for the ULS model in order to consider further influences. Figure 1 shows the structure of the adhesive TLC-concrete composite construction, which serves as the basis for both models. Similarly, the thickness of the individual layers is identical for both models. Table 1 shows the individual layer thicknesses, moduli of elasticity and intrinsic weights for the experiments. For the long-term behaviour tests, a C25/30 concrete and a spruce CLT of strength class C24 were used. The load-bearing tests, on the other hand, used a concrete C40/50 and a CLT of grade C30. The computational models were later validated with the experiments.

Table 1: Layer thicknesses, moduli of elasticity and dead weights for the model ULS and SLS

Layer	Thickness [mm]	Modulus of elasticity [N/mm²]		Density [kN/m³]	
		ULS	SLS	ULS	SLS
concrete	70	35,220	31,476	25	25
adhesive	3	67.2	67.2	-	-
1. CLT layer	40	11,000	12,000	4.2	4.6
2. CLT layer	40	370	400	4.2	4.6
3. CLT layer	40	11,000	12,000	4.2	4.6

4.1. Model – Ultimate Limit Strength

The model for the ultimate limit state is for calculating the stress in the individual layers. It also allows a prediction of the bending stiffness of the composite component, as well as an estimation of the maximum load.

4.1.1. Normal Stress

The normal stress in the single layers is calculated by equation (15) for the normal force component and equation (16) for the bending moment component.

$$\sigma_i = \frac{\gamma_i \, E_i \, a_i \, M}{EJ_{eff}} \tag{15}$$

$$\sigma_{m,i} = \frac{0{,}5 \, E_i \, d_i \, M}{EJ_{eff}} \tag{16}$$

The boundary stress per layer results from the addition of the two terms.

4.1.1. Shear Stress

The shear stress is calculated with the equation (17).

$$\tau_i = -\frac{V_z(x) \, S_y(z)}{J_{eff} \, b} \tag{17}$$

$V_z(x)$ describes the applied lateral force, J_{eff} the effective moment of inertia and $S_y(z)$ the static moment. The static moment depends on the layer which is considered in cross section and varies with the distance z of the single layer to the ideal overall centre of gravity.

4.2. Model – Serviceability Limit Strength

This chapter explains the creation of the SLS model and the effects of temperature, humidity, and time on the deflection of the composite component. The span of the specimen used to validate the model was 4.80 m and the additional load, in addition to its own weight, was 2.21 kN/m². There was no variable load, but additional load was applied later in the long-term study, increasing the overall load to 4.42 kN/m².

The total deformation of the composite section is calculated using equation (18). A positive value means a downward deflection and a negative value means an upward deflection. This is composed of the deformation according to self-weight w_G, additional load w_Q, shrinkage of the concrete w_S, swelling or shrinkage of the CLT slab w_{QS}, and according to the temperature differences between the two building materials wood and concrete w_T together.

$$w(t) = w_G + w_Q + w_S + w_{QS} + w_T \cdot 0{,}05 \tag{18}$$

The temperature deformation is multiplied by a factor of 0.05, since the parameter study has shown that the chosen approach reproduces the course of the vertical deformation well, but in a different order of magnitude. [8]

The deformation due to dead weight and additional load is determined by the same equation (19).

$$w_{G,Q} = \frac{5 \, q_{G,Q} \, l^4}{384 \, EJ_{eff}} \tag{19}$$

4.2.1. Shrinkage and Creep of the Concrete

The deformation w_S due to shrinkage of the concrete is simulated via the equivalent force F_0 and is calculated according to equation (21). The equivalent force follows from the multiplication of the shrinkage strain ε_{cs} with the tensile stiffness EA of the concrete. If the equivalent force is multiplied by the distance a_1 (see equation (20)), the shrinkage moment M_S follows. The distance a describes the distance between the geometric centre of gravity of the concrete slab and the CLT slab.

$$a_1 = a \, \frac{EA_{BSP}}{EA_1 + EA_{BSP}} \tag{20}$$

$$w_S = \frac{M_S \cdot l^2}{8 \cdot EJ_{eff}} \tag{21}$$

The creep of the concrete was determined by ÖNORM EN 1992-1-1 and affects only the modulus of elasticity of the concrete. The creep count is influenced by the temperature, time, and relative humidity of the environment.

4.2.2. Swelling and Shrinkage of CLT

The wood moisture content is calculated using equation (7) in each individual layer. This calculation was performed with the program Wolfram Mathematica 11.1. The CLT slab is hereby divided in total into 12 partial surfaces, whereby each partial surface is one centimetre thick. The layer 0 corresponds to the lower edge of the CLT slab and the layer 12 of the upper edge. For the calculation, however, the humidity was averaged for each layer of the CLT slab, since a varying modulus of elasticity is calculated for these layers. The averaging is done by reading the moisture at the boundaries between the CLT layers. The moisture in layer 1 corresponds to the equilibrium moisture content and depends on the ambient conditions. For layers 4, 8 and 12, the values are read from the Mathematica file. For this purpose, a function is set up according to the time as a function of the input variable - the difference of the equilibrium moisture Δu_{RH} (see Figure 4). The coefficient of diffusion according to Hanhijärvi was used at a constant wood moisture content of $u = 13\%$, which is shown in Figure 4 as greatly exaggerated due to better readability. Although this factor was calibrated on a spruce wood, it is also suitable for the pinewood used in the experiments. Since the density of the pine is slightly higher than that of the spruce, the factor should be slightly lower. However, the exact value of Hanhijärvi was used for the calculation model, because no corresponding values were found in the literature for pinewood. However, the associated error is small because the factors found in the literature for spruce are very different and have a low value.
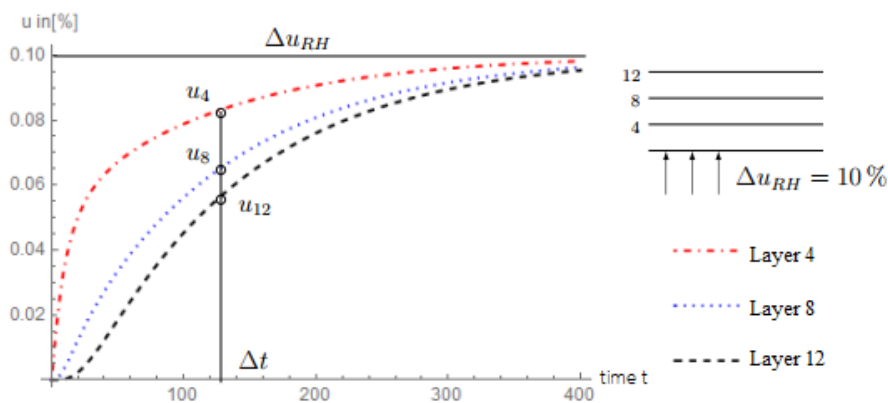

Figure 4: Moisture history in layer 4, 8 and 12 versus time with the increased diffusion factor by Hanhijär-vi (difference of the balance moisture is 10%) [8]

The equilibrium moisture is used as the difference for the calculation. The wood moisture of the 12th layer for measurement n-1 is subtracted from the equilibrium moisture content for measurement n. As only the difference is used for the calculation of the function, the start vector with the constant humidity is set to zero. The schematic sequence is shown by way of example for the calculation of the wood moisture in Table 2.

Table 2: Schematic sequence of the moisture calculation. (1st index = layer, 2nd index = measurement)

Measurement	u_{RH}	Δu_{RH}	Δt	u_1	u_4	u_8	u_{12}	Calculation
0	13 %	0 %	0 h	13,0	13,0	13,0	13,0	u = konst.
1	15 %	2 %	1 h	13,8	13,3	13,0	13,0	$\Delta u_{RH} = u_{RH,1} - u_{12,0}$
2	16 %	3 %	8 h	14,5	14,0	13,1	13,0	$u_{4,2} = u_{4,1} - u_{4,Fkt}$
…	…	…	…	…	…	…	…	
n	$u_{RH,n}$	Δu_n	Δt_n	$u_{1,n}$	$u_{4,n}$	$u_{8,n}$	$u_{12,n}$	

The difference of the equilibrium moisture Δu_{RH} in the second measurement gives a value of 3%. This follows from the calculation of $u_{RH} = 16\%$ minus the moisture in the twelfth layer at the first measurement ($u_{12;1} = 13\%$). In layers 4, 8 and 12, the moisture is read out at the time Δt in the function suitable for Δu_{RH} (see Table 2) and added to the value u_i of the previous measurement. Thus, the value $u_{4;2}$ of the second measurement is calculated from the sum of $u_{4,1}$ of the first measurement and the value u_4 at the time Δt

of the function for the fourth layer at the Δu_{RH} of the second measurement. The functions are stored in Excel with the values of the data points from Mathematica in the respective layers. The data was read into Excel for a time horizon of 720 hours (equivalent to one month).

For the swelling and shrinkage of the CLT slab, the moisture change in the respective longitudinal position is averaged and used to calculate the resulting strain ε_{QS} to:

$$\varepsilon_{QS} = \Delta u \cdot s \tag{22}$$

The shrinkage s of softwood in the longitudinal direction is 0.5% per % change in wood moisture Δu. The distortion ε_{QS} multiplied by the tensile stiffness of the respective layer EA_i gives the force $F_{QS,i}$ which arises as a result of swelling or shrinkage of the wood in the position of the CLT slab. The moment M_{QS} acting on the composite section is calculated from the sum of the forces $F_{s;i}$ multiplied by their distances a_i to the center of gravity of the concrete:

$$M_{QS} = \sum_{i=1}^{2} F_{QS,i} \cdot a_i \tag{23}$$

Therein a_i describes the geometric distance between the centre of gravity of the layer i of the CLT plate to the centre of gravity of the concrete slab. The deflection due to the swelling or shrinkage of the CLT is calculated exactly the same as before the deflection due to shrinkage of the concrete (see equation (21), only the moment M_S is replaced by M_{QS}.

4.2.3. Temperature Change

A change in temperature leads to an expansion or compression of the concrete and the wood. Since these materials have different linear thermal expansion coefficients α_T ($\alpha_T^{concrete} = 12 \cdot 10^{-6}$ [K^{-1}]; $\alpha_T^{timber} = 3,75 \cdot 10^{-6}$ [K^{-1}]), there is a difference in expansion of the two building materials, and subsequently, to the deflection of the composite cross-section. As the temperature increases, the concrete expands more than the underlying CLT. As a result, the composite cross-section is bent upwards and there is a further reduction in the deflection. Similarly, a concrete slab heated at the top can be considered, which leads to the same effect. If, conversely, the temperature decreases, then the concrete shortens more than the CLT, which in turn leads to an increase in the deflection of the composite component. The separate strains of the individual building materials are calculated to:

$$\varepsilon_{T,i} = \alpha_{T,i} \cdot \Delta T \tag{24}$$

If a temperature increase occours, the temperature change ΔT is positive. The difference in the thermal expansions between concrete and CLT is multiplied by the tensile strength of the concrete EA_1:

$$F_T = \left(-\varepsilon_{T,1} + \varepsilon_{T,2}\right) \cdot EA_1 \tag{25}$$

Since an increase in the temperature leads to a greater expansion of the concrete than that of the CLT and an upward bend (negative deflection), the expansion of the concrete must be set negative. The expansion of the CLT is subtracted from the concrete expansion. By multiplying the distance a_1 (see equation (20)) by the force F_T, the moment due to the temperature change M_T is calculated. Finally, with moment M_T, the deflection is calculated as in equation (21).

5.   Validation of the Calculation Models

In the following, the test results of the directly bonded specimens are compared with the calculation results of the two models. In the process, the deviations are discussed in more detail and approaches are reconsidered or, where necessary, analytically adapted.

5.1. Model – Ultimate Limit Strength

The ULS model is used to estimate the load bearing capacity of adhesive CLT-concrete composite elements. In order that the 4-point bending test can be reproduced accurately, the load in the computer program is gradually increased and the deformation in the centre of the plate is continuously calculated. The load is successively increased, and the stresses are evaluated in the layers until one of the maximum allowed stresses of the three materials is exceeded. These maximum allowed stress values correspond to the charac-teristic mean values of the building materials.

The recalculation of the experimental tests in Figure 5 shows that the CLT-concrete composite element is too rigid. However, since the input parameters are not known exactly, each are increased or decreased by 20%, while the other parameters remain at the initial value. A reduction of the modulus of elasticity of the CLT 20% already gives the course from the experiments very accurately. A change in the shear modulus of the adhesive or the CLT has only a minor effect on the overall rigidity of the construction and is not depicted in Figure 5.
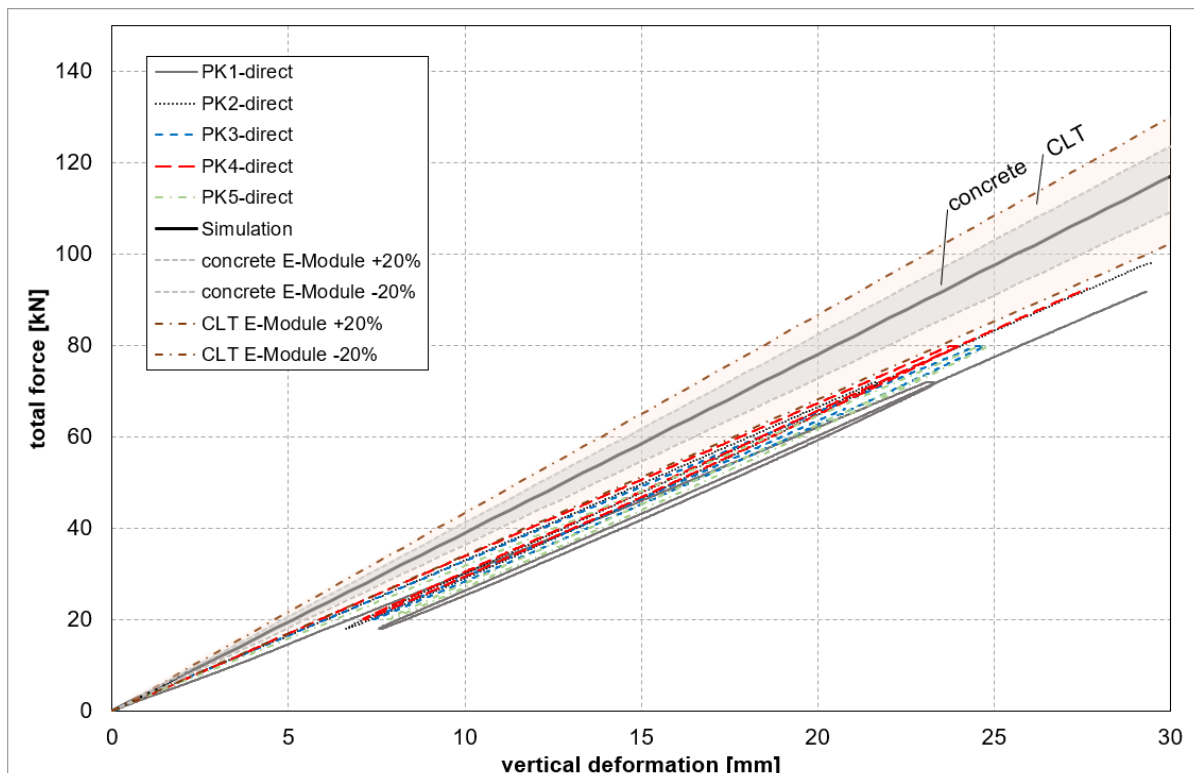

Figure 5: Comparison of results from the calculation model and the load-bearing test of directly bonded spec-imens

The comparison between the mathematical model and the test results of the directly bonded specimens in Figure 5 shows that the γ-method depicts the specimen too stiff. The difference in the deformations between the mean value from the tests (= 100%) and the simulation at 10% and 40% of the maximum load is on average 14%.

Thus, the calculation model with the gamma method is not as accurate because the loads are overestimated. This is due to the fact that the exact input parameters of the calculation model, such as the rolling shear modulus of the CLT or the modulus of elasticity of the concrete are not known precisely. When varying the parameters, however, it becomes apparent that the course can be reproduced fairly accurately. In addition, the γ-method is not optimal for two single loads, since the derivation assumes a sinusoidal load.

5.2. Model – Serviceability Limit Strength

The comparison of the calculation results from the computer model SLS with the measurement results of the sample specimens, which were completely bonded, is shown in the left figure of Figure 6.
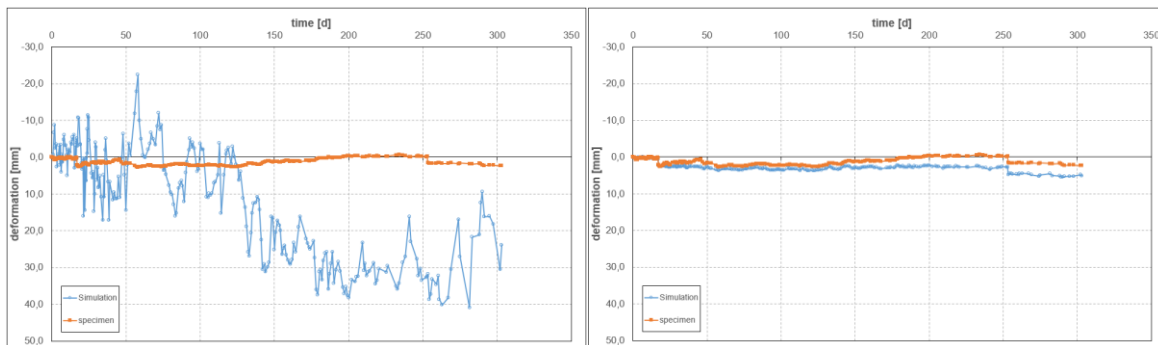

Figure 6: First comparison of results gained by the calculation model and by the experiment
(left: without adapted values; right: without machano-sorptive parts)

First of all, there is a strong deviation between the model and the experiment, and the calculation model does not satisfactorily reflect the deformations of the experiment. The reason is the detection of the mechano-sorptive strain. This is calculated too high with the initially selected model approach and thus falsifies the result. If the mechano-sorptive strain is set to zero and the irreversible strain neglected, the simulation shows a similar, albeit downwardly shifted, deformation curve (see right figure in Figure 6).

Since the deformation curve still has a large deviation, the creep factor of the CLT was set to zero, as the chosen approach is not suitable for a creep calculation of the CLT. This is because the creep number already has the value 1.0 for the first time after a few days and fluctuates very strongly. This approach shows a further improvement of the deflection result, but the reduction of the deformation in the winter months is still not well understood, whereby there is already a certain similarity in the deformation lines between test and simulation. To achieve an even better approximation, the shrinkage deformation of the concrete is multiplied by a factor of 0.5. This can be explained by the addition of additives in concrete production in the precast plants which reduce the shrinkage process by up to 50%. The average deviation between the predicted and the real deformation of the composite is now 126% and the median 51% based on the experiment. These values make clear that the long-term influences with the selected approaches are not suitable for the exact simulation of a long-term test.

However, a better approximation of the deflection is achieved if the long-term behaviour of the concrete - both the shrinkage and the creep - is completely disregarded. This can be justified by the short period of observation, because in this period any creep deformations do not yet occur in size, as the calculation according to the standard suggests. The complete elimination of the deformation due to concrete shrinkage can in turn be attributed to the fact that the precast concrete slab was stored for a certain time until it was connected to the CLT slab. During this period, the shrinkage process of the precast concrete slab was almost completed, as a result of which there was no longer any noticeable shrinkage of the concrete at the composite cross-section.

The course of the deformation at the beginning as well as substantial increases and decreases are now very well reflected by the calculation model. However, the deformation decrease in the period of 130 to 250 days is not detected in the size as it occurs in reality. The deformation increases at the initial load and at the increase of the load will now be almost exactly reproduced in terms of size. Further improvement in the result is possible when the shear modulus of the adhesive is increased. In shear tests, the mean shear modulus was 24 N/mm². In comparative compression tests, a modulus of elasticity of 475 N/mm² was determined, which corresponds to a shear modulus of 170 N/mm² for a transverse expansion coefficient of 0.4. The shear modulus was therefore increased from 24 to finally 97 N/mm². This corresponds to the average of 24 and 170 N/mm². In this final variant (see Figure 7), the average deviation has decreased by 82%. The deviation between

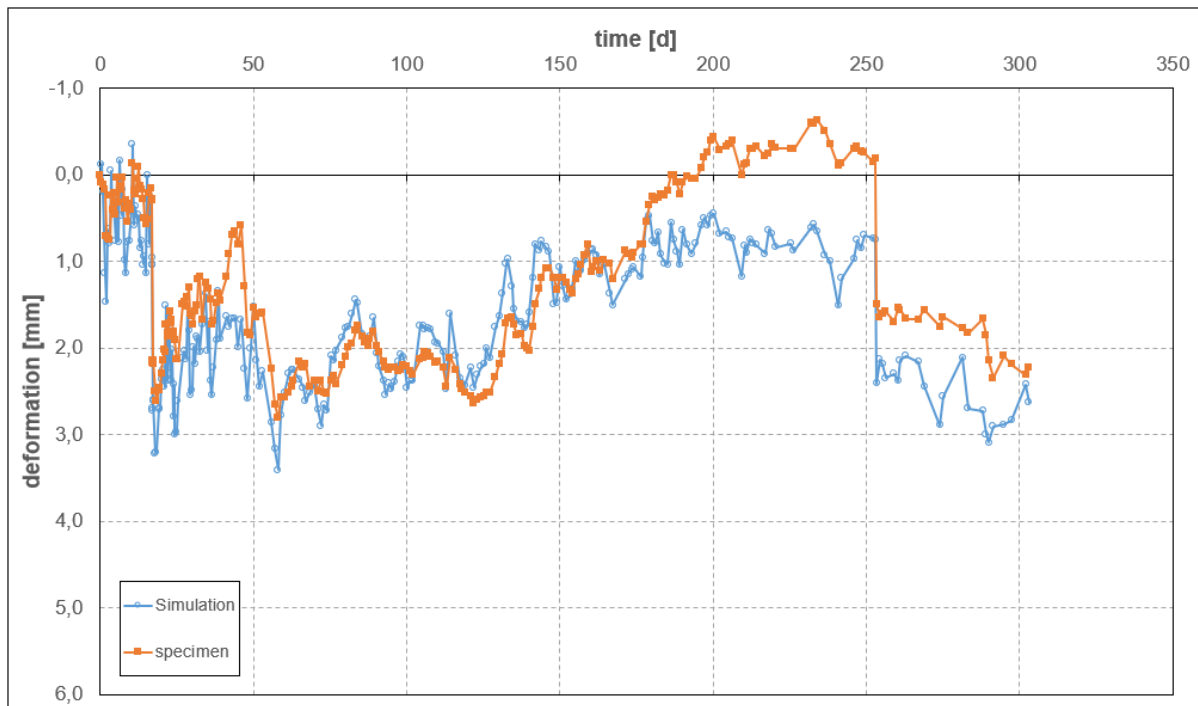the prediction by the calculation model and the real experiment is now 44% and the median at 8% deviation.

Figure 7: Comparison of experimental and simulation results disregarding the creep of the CLT element and the time-dependent behaviour of the concrete (creep and shrinkage). The shear modulus of the adhesive was increased to 97 N/mm².

In summary, for the model SLS for the bonded composite element, it can be said that the initial deformation is reproduced very well, but the strong reduction in deflection with the model is not yet adequately captured. The reason for this could be that the assumed coefficient of diffusion of Hanhijärvi differs significantly from the value occurring in reality. At the end of the experiment, the difference between measurement and simulation was 0.4 mm, which corresponds to a deviation of 18% (test = 100%).

6.   Conclusion

In this work, two calculation models for adhesive CLT-concrete composite elements were presented. The model validation shows that the γ-method with the additional approaches chosen in this work is only conditionally suitable for an exact prediction of the long-term behaviour. It should be noted, however, that the results of the computational model depend very much on the input parameters and that they were not all accurately known or could not be determined from the real experiments. The simulation of the carrying capacity with the γ-method certainly shows potential, but this is also very much dependent on the model input parameters. In general, the variant of the adhesive CLT-concrete composite construction can be classified as very viable and efficient. For the long-term behaviour, longer test periods are necessary in order to be able to make a reliable statement about the creep behaviour and subsequently about the creep factor of the construction. For an adequate calculation model, the most accurate determination of the input parameters is of the utmost importance. Nonetheless, the models presented here are suitable for pre-dimensioning adhesive wood-concrete composite floors, as well as estimating the load and deflection.

7. Literatur

[1] *Möhler, K.:* Über das Tragverhalten von Biegeträgern und Druckstäben mit zu-sammengesetzten Querschnitten und nachgiebigen Verbindungsmitteln. TH Karlsruhe, Habilitation, 1956.

[2] *Fernandez-Cabo, J.L.; Fernandez-Lavandera, J.; Diez-Barra, R. et al.:* The flexibility matrix of timber composite beams with a discrete connection system.

[3] *Wallner-Novak, M.; Koppelhuber, J.; Pock, K.:* Brettsperrholz Bemessung – Grundlagen für Statik und Konstruktion nach Eurocode, pro:Holz Information,, 2013.

[4] *Hanhijärvi, A.:* Modelling of creep deformation mechanisms in wood. Espoo, Helsinki University of Technology. Technical Research Centre of Finland., Dissertation, 1995.

[5] *Fortuin, G.:* Anwendung mathematischer Modelle zur Beschreibung der techni-schen Konvektionstrocknung von Schnittholz. Hamburg, Universität Hamburg, Dissertation, 2003.

[6] *Eisenhut, L.:* Geklebter Verbund aus Holz und hochfestem Beton - Untersuchungen zum Langzeitverhalten, Schriftenreihe Bauwerkserhaltung und HolzbauHeft 7, Kassel University Press, Kassel, Hess, 2016.

[7] *Fortino, S.; Mirianon, F.; Toratti, T.:* A 3D moisture-stress FEM analysis for time dependent problems in timber structures. *In:* Mechanics of Time-Dependent Materials 13 (2009), Heft 4, S. 333-356.

[8] Georg Erlinger: Rechenmodelle für geklebte Holz-Beton-Verbundkonstruktionen. Wels, University of Applied Sciences Upper Austria, Masterarbeit, 2019.